Multifaceted approach for evaluating peripheral neurotoxicity in isoniazid-treated rats

末梢神経毒性を正確に評価するための イソニアジド投与ラットを用いた多角的アプローチ

2024 年 2 月

麻布大学大学院　獣医学研究科

獣医学専攻　博士課程

DV2004　　樫村　茜

Abstract

In drug development, assessment of non-clinical peripheral neurotoxicity is important to ensure human safety. Clarifying the pathological features and mechanisms of toxicity enables the management of safety risks in humans by estimating the degree of risk and proposing monitoring strategies. Published guidelines for peripheral neurotoxicity assessment do not provide detailed information on which endpoints should be monitored preferentially and how the results should be integrated and discussed.

To identify an optimal assessment method for the characterization of peripheral neurotoxicity, we conducted pathological, biochemical (biomaterials contributing to mechanistic considerations and biomarkers), and behavioral evaluations of isoniazid-treated rats. We found a discrepancy between the days on which marked pathological changes were noted and those on which biochemical and behavioral changes were noted, suggesting the importance of combining these evaluations. Although pathological evaluation is essential for pathological characterization, the results of biochemical and behavioral assessments at the same time points as the pathological evaluation are also important for discussion. In this study, since the measurement of serum neurofilament light chain could detect changes earlier than pathological examination, it could be useful as a biomarker for peripheral neurotoxicity. Moreover, examination of semi-thin specimens and choline acetyltransferase immunostaining were useful for characterizing morphological

neurotoxicity, and image analysis of semi-thin specimens enabled us to objectively show the pathological features.

Contents

General Introduction

Drug-induced peripheral neuropathy is often reported in non-clinical and clinical studies during the drug development process. Accurate assessment of peripheral neurotoxicity in non-clinical studies is important to ensure human safety. An assessment to characterize the pathophysiology and to elucidate the mechanism of peripheral neurotoxicity enables us to manage the safety risk in humans through estimation of the degree of risk and proposal of monitoring strategies. Published guidelines (Organisation for Economic Co-operation and Development [OECD] guidance and review articles) for peripheral neurotoxicity assessment do not provide detail information on which endpoints should be monitored preferentially and how the results should be integrated and discussed[1-5]. In the early stage of drug development, observation items for evaluating the neurotoxicity may not be designed in the screening studies to select better candidates. The battery for evaluating neurotoxicity is sometimes included in the general toxicology studies, however, it is often difficult to set a complete panel of measurement parameters and observation items for the test article with unknown toxicological profile. Therefore, it is important to detect a possible neurotoxicity of candidates at an early stage for further development of selected candidates. Meanwhile, non-clinical neurotoxicity assessment, particularly for peripheral neurotoxicity, is complicated by the following issues: (1) lack of established peripheral neurotoxicity biomarkers (BMs); (2) lack of clarity regarding which

behavioral evaluation should be conducted; (3) Unestablished standard method for objective measurement of pathologic toxicity features; and (4) difficulties for choice of appropriate necropsy time points.

In drug development, humoral BM can be used in both non-clinical and clinical studies as required. A BM with a high sensitivity is useful for neurotoxicity monitoring in humans[6]. Neurofilament light chain (Nf-L) is a protein component of neurons that is being established as a humoral BM of axonal injury reflecting central neurodegenerative disease and traumatic brain injuries[7-9]. In recent years, the NF-L has been attracting attention also as a humoral BM of peripheral nerve injury[6, 10]. There are publications to have detected significant increase in serum Nf-L level in rats with peripheral nerve injury[11-13].

Isoniazid (INH), an anti-tuberculosis drug, is known to induce peripheral neurotoxicity due to vitamin B6 (VB6) deficiency[14]. The main circulating forms of VB6 are pyridoxal (PL) and its active form, pyridoxal phosphate (PLP), and these are detectable in plasma. According to the review articles, it was suggested that INH inhibits pyridoxal phosphokinase (PDXK), an enzyme that converts PL to PLP, resulting in PLP depletion and peripheral neuropathy[14-15]. However, the association between serum PLP levels and neurotoxicity is not well established[16]. It is difficult to detect a decrease in plasma VB6 level uniformly in humans because of the large variation in dietary intake of VB6 among individuals, and no study in laboratory animals has

compared the time course of the plasma VB6 level with the time course of toxic changes. Peripheral neurotoxicity due to INH treatment is considered distal axonal degeneration[17-18], and several reports have provided a detailed pathological examination of the morphological changes over time[17, 19-20]. However, whether these changes due to PLP deficiency are located mainly in the sensory or motor neurons has not been clearly determined[16, 21-23]. In clinical, these changes may initially occur in sensory nerves but may later show signs of motor dysfunction[24-25].

To find an optimal assessment method for the characterization of peripheral neurotoxicity, we conducted not only pathological evaluations but also biochemical and behavioral evaluations in INH-treated rats. And we discussed the combination of the pathological results and the other results. In this study, we designed to effectively narrow down the neurotoxicity endpoints in the early stage of drug development, and the usefulness of each endpoint was discussed.

General Materials

Animals

Five-week-old male Sprague Dawley (Crl:CD) rats were purchased from Charles River Laboratories Japan (Kanagawa, Japan) and used at 6 weeks of age. Sprague Dawley rats are the standard strain used in general toxicity studies. INH (Cat No. I3377, Sigma-Aldrich) was dissolved in 0.5% (w/v) methylcellulose (Sigma-Aldrich)- 0.3% (w/v) Tween®80 (Sigma-Aldrich) solution and administered by oral gavage for 3 days at 0 (vehicle control), 250, and 500 mg/kg/day. Day 1 was defined as the first day of dosing. Animals were sacrificed by exsanguination under deep anesthesia with an inhalation of isoflurane on Days 4, 9, and 30. The dose and the timing of necropsy were determined on the results of a preliminary study performed with a similar time course at 300, 500, and 1000 mg/kg/day. The 1000 mg/kg/day group showed severe body weight loss, and the 500 mg/kg/day showed sufficient peripheral neurotoxicity. The detailed group composition is shown in Table 1. All animals were fasted from the evening prior to the necropsy day (Days 3, 8, and 29). Blood was collected for each examination from the posterior vena cava of animals under anesthesia. Necropsies, including macroscopic observations of the external surface and the organs in thoracic and abdominal cavities, were performed. After transcardiac perfusion with 4% paraformaldehyde, the brain, spinal cord (including dorsal root ganglion [DRG]), sciatic nerve, tibial nerve, and saphenous

nerve were collected. Tissues were immersed in 10% neutral buffered formalin, and part of the sciatic nerve was fixed in 2.5% glutaraldehyde for electron microscopy. All procedures were endorsed by the Institutional Animal Care and Use Committee of the test facility (Application No. TAT190185) and performed in accordance with animal welfare and Mitsubishi Tanabe Pharma Corporation's internal rules for proper conduct of animal experiments.

Table

Table 1. Composition of the animal groups.

Group No.	Necropsy day	INH dose (mg/kg/day)	Dose volume (mL/kg/day)	Dose concentration (mg/mL)	Number of animals (Animal #)
1	Day 4	0	5	0	5 (10101-10105)
2	Day 4	250	5	50	5 (10201-10205)
3	Day 4	500	5	100	5 (10301-10305)
4	Day 9	0	5	0	5 (10401-10405)
5	Day 9	250	5	50	5 (10501-10505)
6	Day 9	500	5	100	5 (10601-10605)
7	Day 30	0	5	0	5 (10701-10705)
8	Day 30	250	5	50	5 (10801-10805)
9	Day 30	500	5	100	5 (10901-10905)

Chapter 1: Behavioral evaluations

Methods

Endpoints in living animals

All animals were observed for clinical signs once daily. The observations for clinical signs are the usual methods used in toxicity and pharmacology studies. Body weight and food consumption were measured on Days 1 - 9, 11, 14, 18, 21, 25, and 29.

As behavioral evaluations, a thermal sensation test (hot plate method) and detailed symptom observation (selected items from the modified Irwin's test: locomotor activity, body posture, ataxic gait, abnormal gait, abdominal muscle tone, trunk muscle tone, limb muscle tone, ipsilateral flexor reflex, grip strength, pinna reflex, corneal reflex, and pain reaction[26-27]). The thermal sensation test is mainly used in pharmacological evaluation to determine the effect on sensory function by confirming the blunting to thermal sensory stimulation. The detailed symptom observation is more likely to detect changes than observation for clinical signs, and skilled toxicologists can easily conduct the observation because it is usually used for safety pharmacology evaluation. These evaluations were performed on Days -1, 3, 8, and 18. The tests were not performed on Day 29 because there was no change on Days 8 and 18. On Days 4, 5, 6, 9, and 30, the ipsilateral flexor reflex of the hindlimb was also assessed (Fig. 1). For the thermal sensation test, after a rat had 2 minutes of acclimation on a hot plate at room temperature, we

measured the latency (seconds) to perform avoidance behavior when it was placed on a hot plate at approximately 53℃. The test was performed in duplicate to confirm reproducibility. The judgment of avoidance behavior was made by the observer based on the manifestation of the following behaviors: licking, rearing, tapping, or jumping. The latency ≧ 10 seconds in both of the duplicate measurements was recorded as an abnormality because the latencies on Day -1 and in the control group were < 10 seconds.

Hematology and blood chemistry

For hematology analysis, blood samples collected into anticoagulant (EDTA-2K)-coated tubes. The following parameters were measured with an automated analyzer (Automated Hematology Analyzer XT-2000iV, Sysmex Corporation, Kobe, Japan): erythrocyte count (RBC), hemoglobin concentration (Hb), hematocrit (Ht), mean corpuscular volume (MCV), mean corpuscular hemoglobin (MCH), mean corpuscular hemoglobin concentration (MCHC), red cell distribution width (RDW-SD), reticulocyte count and ratio (RET), platelet count (PLT), mean platelet volume (MPV), leukocyte count (WBC), and differential leukocyte count and ratio (lymphocytes, neutrophils, monocytes, eosinophils, and basophils).

For blood chemistry analysis, serum was obtained from the collected blood samples. The following items were measured with an automated analyzer (Hitachi Automatic Analyzer

LABOSPECT 006, Hitachi High-Tech Corporation, Tokyo, Japan): aspartate aminotransferase (AST), alanine aminotransferase (ALT), glutamate dehydrogenase (GLDH), alkaline phosphatase (ALP), total bilirubin (TBil), direct bilirubin (Dbil), indirect bilirubin (Ibil; calculated from Tbil and Dbil), total bile acid (TBA), urea nitrogen (UN), creatinine (CRE), glucose (Glu), total cholesterol (TC), triglycerides (TG), total protein (TP), albumin/globulin ratio (A/G), calcium (Ca), inorganic phosphorus (IP), sodium (Na), potassium (K), and chloride (Cl).

Statistical analysis

Dunnett's multiple comparison test was performed on the data of hematology parameters and blood chemistry parameters. All significance levels were two-sided, 5%.

Results

Endpoints in living animals including behavioral findings

There were no marked changes in clinical signs and necropsy findings. Dose-dependent body weight loss or suppression of body weight gain was observed during the dosing period and was associated with decreased food consumption; however, the changes recovered promptly after the dosing period (Fig. 2).

In the behavioral assessment, delayed time from placement on a hot plate to avoidance behavior was observed in 2 of 15 animals of the high-dose group on Day 3. No abnormality was noted on Day 8. Mild hyporeflexia of the ipsilateral flexor muscle of the hindlimb was observed in 3 of the 15 animals in the high-dose group on day 4. One of these animals showed the similar change on day 5. No changes were observed in the behavioral evaluation conducted from Day 6 onward. (Table 2).

Hematology and blood chemistry

In the hematology analysis, reticulocytes decreased dose-dependently on Day 4 and increased on Day 9 in the high-dose group (Fig. 3). The decrease on Day 4 was considered a transient change associated with the body weight decrease during the dosing period, and the increase on Day 9 was considered its rebound effect.

In the blood chemistry analysis, the following findings were noted on Day 4 (Fig. 3): Cl increased

slightly in the high-dose group and was associated with the body weight decrease. There were mild increases in GLDH, UN, and CRE.

Discussion

In the behavioral evaluation, evaluating the ipsilateral flexor reflex was considered useful. It could detect behavioral abnormalities that could not be detected by general clinical observation. Although the incidence was low, this change was considered to be related to neurotoxicity rather than a worsening of the condition. In our previous study (data not shown), 6-week-old Sprague Dawley rats given 25% restricted feeding for 3 days showed marked body weight loss, emaciation, and low reticulocyte count, but no effects on activity or behavior. In addition, it may be easy to include in general toxicity studies and could be evaluated daily, because it is easy to check and places less stress on the animals. Although abnormalities were detected in the thermal sensory stimulation test as well, it was considered difficult to incorporate in the toxicity evaluation because it was difficult to judge the change by subjective observation, and it took a long time for acclimation and evaluation. It is also a disadvantage that the effect target is often unknown in general toxicity studies, unlike pharmacology studies, so sensory abnormalities other than thermal stimulation may not be detected. The small number of animals with changes in both evaluations was considered to be due to possible differences in severity between animals and the possibility that symptoms may not appear if there are more than a certain number of nerve fibers with residual function.

In blood chemistry, mild increases in the GLDH, UN, and CRE levels were observed, suggesting transient

hepatorenal dysfunction. INH is known to cause various injuries due to VB6 deficiency, including hepatic and renal disorders. However, these changes were not considered to interfere with the evaluation of peripheral neurotoxicity because the event was transient and the results had returned to normal by Day 9 and thereafter.

Figures and Tables

Figure 1. The ipsilateral flexor reflex of the hindlimbs. When the hindlimb is extended caudally, the flexor reflex normally causes the hindlimb to flex back into original position.

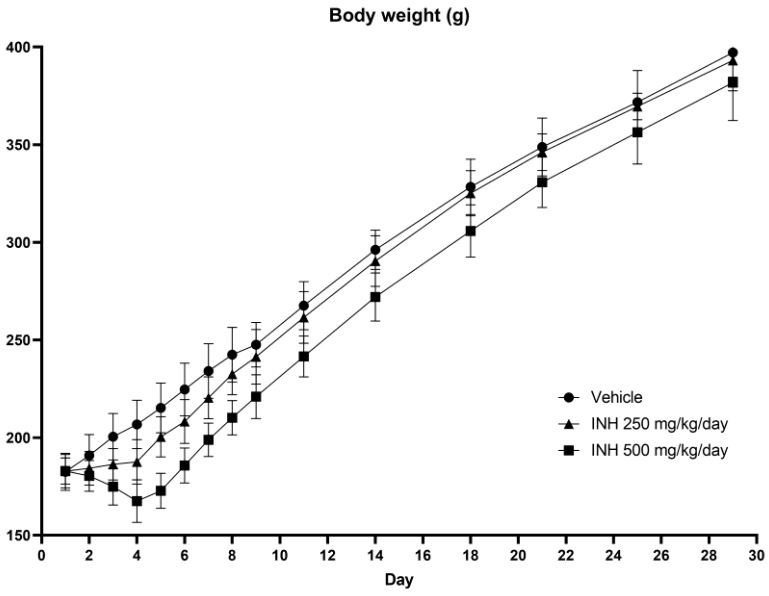

Figure 2. Average body weight from Day 1 to Day 29. Dose-dependent weight loss or suppression of weight gain was observed until Day 4 (the day after the end of isoniazid [INH] dosing); however, body weight recovered after Day 5. Error bars indicate standard deviation.

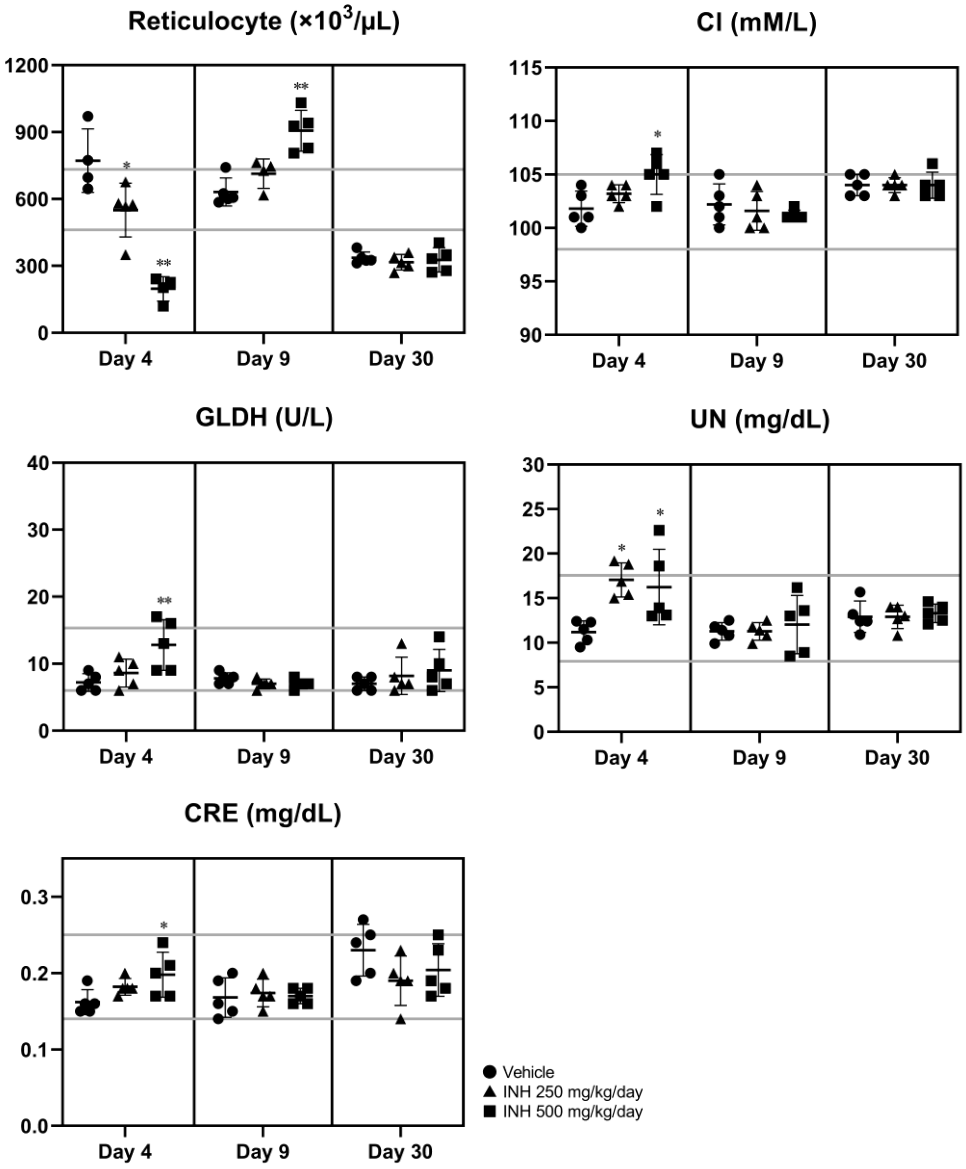

Figure 3. Hematology and blood chemistry at necropsy. Values on the vertical axis are facility data from normal 7-week-old rats (2.5–97.5 percentile, n=109). Reticulocytes were decreased dose-dependently on Day 4 and increased on Day 9 in the high-dose isoniazid (INH) group. Chloride (Cl) was increased slightly in the high-dose group on Day 4. Mild increases in glutamate dehydrogenase (GLDH), urea nitrogen (UN), and creatinine (CRE) were noted. Significant differences, compared with the vehicle group, are shown (*P<0.05, **P<0.01). Error bars indicate standard deviation.

Table 2. The summarized results of behavioral assessment.

Assessment	Days 3-5			Days 8-9			Day 30		
Findings	Vehicle	INH low	INH high	Vehicle	INH low	INH high	Vehicle	INH low	INH high
Ispilateral flexor reflex[a]									
Mild hyporeflexia of the hind limb	-	-	P (3/15)[b]	-	-	-	-	-	-
Thermal sensitivity test[c]									
Delayed time from placement on a hot plate to evading behavior	-	-	P (2/15)	-	-	-	NA	NA	NA

Descriptions in parentheses: number of animals with findings/number of animals examined.
INH low: INH 250 mg/kg/day for 3 days, INH high: INH 500 mg/kg/day for 3 days.
-: no noteworthy findings, P: present, NA: not appreciable.
a: Ipsilateral flexor reflex was examined on Days 3 - 6, 8 - 9, and 30.
b: Mild hyporeflexia of the hind limb was noted in 3 of 15 animals on day 4, and in 1 of 10 animals on day 5. It was not noted on day 3 and after Day 6.
c: Thermal sensitivity test was performed on Days 3 and 8.

Chapter 2: Biochemical Evaluations

Methods

Serum Nf-L measurement

Serum was obtained from the collected blood samples. The serum samples of 3-5 animals per each group (except for Group 8) were used to obtain the Nf-L concentration. Serum Nf-L concentrations were measured using a Simoa HD-X analyzer (Quanterix, Massachusetts) with a Simoa NF-light V2 Advantage Kit (Cat No. 104073, Quanterix) according to the manufacturer's instructions. For measurement validation, the accuracy of the calibration curve, concentration of quality control (QC) samples, intra-assay and inter-assay reproducibility, and dilution parallelism were confirmed. Also, for the measurement batch, data that met the criteria for the accuracy of the calibration curve and concentration of QC samples were adopted.

Plasma VB6 measurement

Plasma was obtained from blood samples collected into anticoagulant (EDTA-2K)-coated tubes. To prepare standard solutions, we made serial dilutions of pyridoxal hydrochloride for PL, pyridoxal 5 -phosphate monohydrate for PLP, and heptafluorobutyric acid purchased from Sigma-Aldrich (MO, US). The concentrations of the prepared standard solutions are shown in the calibration curve range in Supplementary Table 1. The internal standard (IS) solutions were

prepared by diluting the stock solutions of pyridoxal hydrochloride methyl-D3 and pyridoxal 5'-phosphate methyl-D3 purchased from Buchem B.V. (Apeldoorn, NL) to 100 nM and 75 nM, respectively. Plasma samples, trichloro acetic acid solution, and the IS solution of the stable isotope for each analyte were mixed to precipitate plasma proteins. The centrifuged supernatant was used as the analysis sample. The standard solutions were processed in the same manner and used as the calibration curve standards.

PL and PLP were measured individually on a liquid chromatography–tandem mass spectrometry (LC-MS/MS) system. The system was composed of the Prominence series (Shimadzu Corporation, Kyoto, Japan), Nexera X2 series (Shimadzu Corporation, Kyoto, Japan) and Qtrap 4500 system (AB Sciex, MA, US). Analyst, version 1.6.2 (AB Sciex, MA, US), was used to control the instrument and for data acquisition. PL was separated on an Acquity HSS-T3 guard column (1.8 μm, 2.1 mm × 5 mm, Waters, MA, US) and Acquity HSS-T3 analytical column (1.8 μm, 2.1 mm × 100 mm, Waters, MA US). PLP was separated on an Acquity HSS-T3 guard column (1.8 μm, 2.1 mm × 5 mm, Waters, MA, US) and InertSustain C18 (1.8 μm, 2.1 mm × 100 mm, GL Sciences Inc., Tokyo, Japan). Both analytes were eluted using a gradient mobile phase system consisting of two components. The mass spectrometer was operated in the positive MRM mode with a dwell time set at 100 ms. Analyte-specific settings are shown in Supplementary Table 1.

Statistical analysis

Dunnett's multiple comparison test was performed on the data of serum Nf-L measurement and plasma VB6 measurement. All significance levels were two-sided, 5%.

Results

Serum Nf-L levels

Serum Nf-L levels were measured to confirm the utility of Nf-L as a humoral BM (Fig. 4). On day 4, serum Nf-L levels were increased markedly in a dose-dependent manner, but the increase was not statistically significant because of inter-individual variability. On day 9, the levels were increased with less variation than on day 4, and the increase was statistically significant in the high-dose group. On day 30, the levels of both treatment groups were comparable to those of the control group.

Plasma concentrations of PL and PLP

To investigate the possible relationship between VB6 levels and neurotoxicity caused by INH treatment, plasma concentrations of PL, as well as its activated phosphorylated form PLP, reflecting the tissue stores of VB6[16], were measured. A marked dose-dependent decrease in both the PL and PLP levels was observed on day 4; however, no decrease was observed after day 9 (Fig. 5). The decrease in plasma VB6 levels rapidly recovered after the dosing period.

Discussion

The usefulness of Nf-L as a peripheral neurotoxic BM was suggested for the detection of nerve fiber injury. Serum Nf-L measurement is non-invasive and useful for monitoring toxicity in humans as well. Even at the early stage when it is difficult to detect clear morphological changes and the degree of lesions is likely to differ among individuals, changes can be detected even with a small sample size because the serum Nf-L levels are expected to be markedly high by nerve injury. As Nf-L cannot distinguish between neuronal damage in the central nervous system (CNS) and the peripheral nervous system, concomitant evaluation of the CNS is required.

In another type of bioanalysis, plasma PL and PLP levels were measured. Both decreased on Day 4 and recovered on Day 9 when nerve fiber degeneration was prominent. In INH-induced peripheral neurotoxicity, it was confirmed that VB6 deficiency occurs in the early stage of injury. In the report by Chua et al, the PLP conversion of VB6 incorporated into nerve tissue occurs mainly in nerve cell bodies, and PLP is transported to axons and used for metabolism[17]. In the PLP-deficient state, the neuron is susceptible to the effect of PLP deficiency on the more distal axon side, and nerve fiber degeneration may have occurred from the distal side in long peripheral axons[17]. Therefore, it is considered likely that it took time for the pathological changes to appear due to the processes of decreased PLP concentration in nerve tissue, transport, and metabolic disorder, which occur after the decrease in plasma PLP level. Changes in plasma PL

and PLP levels at an early stage are useful markers for the early prediction of subsequent peripheral nerve injury induced by INH. We often cannot determine what to measure if there is no mechanistic hypothesis for toxicity, and some endogenous molecules are difficult to measure. However, the measurement of biological substances related to mechanistic hypotheses can provide a useful rationale for discussing toxicity mechanisms.

Figures and Tables

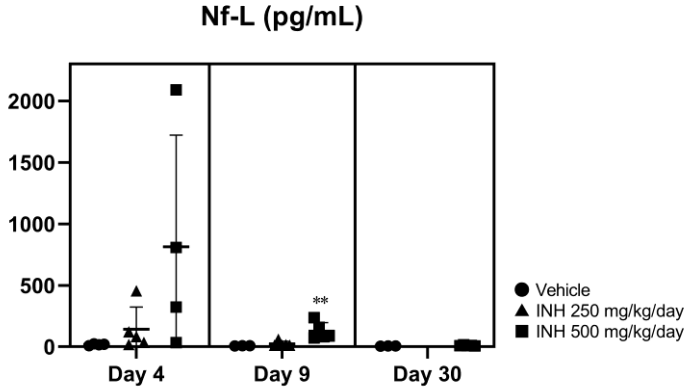

Figure 4. Serum concentrations of neurofilament light chain (Nf-L) at necropsy. Significant differences, compared with the vehicle group, are shown (**P<0.01). Error bars indicate standard deviation.

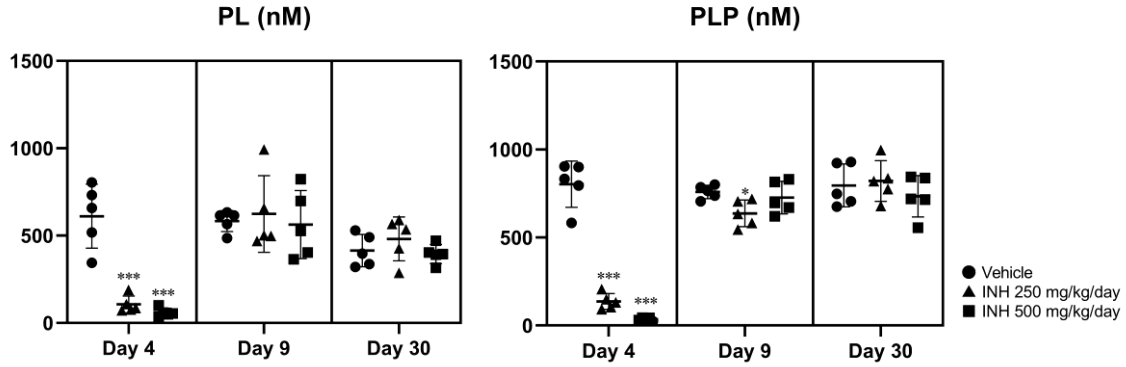

Figure 5. Plasma concentrations of pyridoxal (PL) and pyridoxal phosphate (PLP) at necropsy. Significant differences, compared with the vehicle group, are shown (*P<0.05, ***P<0.001). Error bars indicate standard deviation.

Supplementary Table 1. Analytes, selected MRM transitions, retention time (RT) and parameter settings.

Analyte	Q1 Mass, *m/z*	Q3 Mass, *m/z*	RT (min)	DP (V)	EP (V)	CE (eV)	CXP (V)	Calibration curve range (nM)
PL	167.966	149.9	1.2	11	10	17	12	30-2000
PL-D3 (IS)	170.978	153.1	1.2	6	10	13	12	-
PLP	247.853	149.9	2.5	96	10	21	12	10-1000
PLP-D3 (IS)	250.885	153.0	2.5	91	10	21	12	-

DP, declustering potential; EP, entrance potential; CE, collision energy; CXP, collision cell exit potential.

Chapter 3: Pathological Evaluations

Methods

Histopathological examination of formalin-fixed paraffin-embedded (FFPE) sections

The fixed tissues were dehydrated, embedded in paraffin, and stained with hematoxylin and eosin (HE) by a routine method. The HE-stained sections of the brain, spinal cord (including DRG), sciatic nerve, tibial nerve, and saphenous nerve were prepared for microscopic examination. Peripheral nerves were prepared longitudinally. In addition, for the sciatic nerve, Luxol fast blue (LFB)-Bodian staining was performed for identification of axons and myelin sheaths. These sections were examined microscopically.

For immunohistochemistry, the sciatic nerve sections of 3 representative animals were selected and used for characterizing the nerve fiber degeneration and recovery process observed in the HE sections, from each of the following groups: Group 4 (received 0 mg/kg/day; scheduled sacrifice on Day 9), Group 6 (received 500 mg/kg/day; scheduled sacrifice on Day 9), and Group 9 (received 500 mg/kg/day; scheduled sacrifice on Day 30). After deparaffinization, immunohistochemistry using an anti-choline acetyltransferase (ChAT) antibody (Cat No. Ab178850, Abcam, 1:1000 dilution), an anti-Nf-L antibody (Cat No. M0762, Agilent Technologies, 1:500 dilution) and an anti-ionized calcium binding adapter molecule 1 (Iba1) antibody (Cat No. 019-19741, Fujifilm Wako, 1:2000 dilution) was performed with an automated

staining device (HISTOSTAINER 48A, Nichirei Biosciences Inc., Japan) in accordance with the manufacturer's instructions. We performed heat-induced epitope retrieval with citrate buffer pH6 or Tris-EDTA buffer pH9 and blocking with protein blocking buffer (Block Ace Powder, Cat No. UKB 80, KAC) in accordance with standard procedures. The sections were incubated with primary antibody for 1 hour and with secondary antibody for 30 minutes at room temperature. Immunoreactivity was detected and visualized by performing a peroxidase-diaminobenzidine (DAB) reaction (Peroxidase Stain DAB Kit [Brown Stain], Nacalai Tesque, Kyoto, Japan) before the sections were counterstained with hematoxylin.

Histopathological examination using semi-thin sections

Toluidine blue (TB)-stained semi-thin sections of the sciatic nerve were prepared and examined by light microscopy. For image analysis, whole digital slide images were obtained using virtual microscopy (Aperio AT2, Leica Biosystems, Wetzlar, Germany); then, using HALO image analysis software (v3.64134.166, Indica Labs, Albuquerque, NM, USA) and its Axon module, histopathological features of neuron fibers were analyzed and quantified for all animals. The items measured were as follows: axon count, total area (axon area, nerve fiber area, myelin area, and total tissue area), average diameter (axon diameter and nerve fiber diameter), and average area (axon area, nerve fiber area, and myelin area). A valid analysis method to clarify the

histopathological features was considered to be histogram analysis that can show the distribution of nerve fibers with morphological differences for each individual. To clarify the histopathological features, we used the G-ratio (proportion of axonal diameter in the nerve fiber diameter) data[28] and performed histogram analysis for 2 representative animals selected from each of the following groups: Group 4 (received 0 mg/kg/day; scheduled sacrifice on Day 9) and Group 6 (received 500 mg/kg/day; scheduled sacrifice on Day 9). To verify the accuracy of image recognition of nerve fibers by the software, positive predictive value and sensitivity were calculated by counting the number of nerve fibers and visually comparing the actual stained images with the nerve fibers recognized by the software. 125 μm x 125 μm squares were extracted randomly at 3 sites/animal, and nerve fibers were counted visually.

Ultrastructural examination

To clarify the ultrastructural features of nerve fiber degeneration, the ultrathin sections were prepared for the sciatic nerve of 2 animals per each group according to the conventional method. The sections were electron stained with uranyl acetate and examined. The findings in nerve fibers were compared with the control group, and photographs were obtained with a transmission electron microscope (JEM-1400, JEOL Ltd., Tokyo, Japan).

Results

Histopathological findings of FFPE sections and semi-thin sections

In the histopathological examination using FFPE sections, nerve fiber degeneration was observed in each peripheral nerve as neuropathy caused by INH (Table 3). There were no significant differences in the degree of changes among the sciatic nerve, tibial nerve, and saphenous nerve. Nerve fiber degeneration was observed only sporadically in the high-dose group on Day 4 at the end of dosing, but it was most marked, and observed at a high frequency, on Day 9 (Fig 6). On Day 30, the nerve fiber degeneration recovered, while there were macrophages stained positive for Iba-1 and having foamy cytoplasm, sporadically between nerve fibers (Fig. 6 and 7A). Macrophage infiltrate was considered to be the finding indicative of scavenging character of macrophages to remove the destructed axon and/or myelin components. In HE and LFB-Bodian staining, nerve fiber degeneration was recognized as “digestion chambers” with fragmented axons and spherules derived from the myelin sheath at sites where axons had disappeared (Fig. 6 and 7B). No obvious changes were observed in the brain, spinal cord, and DRG.

In the immunohistochemistry with anti-ChAT antibody, the toxicologically relevant positive reaction was not observed in the degenerated nerve fibers (Fig. 8). ChAT is a marker for cholinergic nerves (autonomic nerves and motor nerves). This result suggested that the axonal

degeneration occurred mainly in sensory nerves in the peripheral nerves.

Light microscopic observation of the TB-stained semi-thin specimens were also performed, and the results are shown in Table 4. In animals with severe pathology, blue stained myelin ovoids were frequently observed, and morphological variability (unequal size or irregular shape) of each nerve fiber was also observed (Fig. 9A). The myelin ovoids were caused by a winding proliferation of the myelin sheath that occurred after the axons were damaged and lost. This finding was also observed on Day 4 in the low-dose group without any findings in the observation of the FFPE specimens. The unequal size of nerve fibers was thought to result from changes such as expansion of axons associated with axonal injury (considered to be caused by proliferation of intracellular organelles), enlargement of nerve fibers caused by reactive changes in the myelin sheath, and appearance of small nerve fibers for regeneration.

Image analysis of semi-thin sections

We used the HALO software to distinguish axons from myelin sheaths and to quantify the diameter and area of each nerve fiber. Based on the obtained values, we evaluated the G-ratio (axonal diameter/nerve fiber diameter) using a histogram as a distribution of the number of nerve fibers[28]. In the histogram of the animals received INH 500 mg/kg/day compared with that of the vehicle-treated animals, the increased myelin ovoids in the sections of the INH-treated animals

showed a marked increase in the G-ratio 0 value. In addition, the variability in nerve fibers was shown as a decreased G-ratio distribution and a slight increase in the G-ratio 0.6–0.8 value (Fig. 9B). The validity of image recognition was demonstrated by visually counting nerve fibers and calculating the positive predictive value and sensitivity of nerve fiber recognition. Both the positive predictive value and sensitivity were greater than 90% (Supplementary Table 2).

Ultrastructural findings

In the ultrastructural examination, a time-course change in axonal degeneration was observed (Fig. 10). On Day 4, disruption of axon and myelin sheath were observed as early signs of axonal injury, and axonal disintegration-associated myelin ovoids were occasionally present. On Day 9, axonal degeneration, disruption of myelin sheath, and myelin ovoid formation with loss of axons were observed in many nerve fibers, and enlargement of Schwann cell, hypermyelination, increase in small myelinated fiber were observed as reactive changes. On Day 30, the frequency of small nerve fibers with thin myelin sheaths, indicative of their repairment process, increased.

Discussion

The pathological features of the nerve fiber degeneration observed in this study were similar to those reported in the literature with morphological evaluation of INH-induced peripheral neurotoxicity[17, 19-20].

In the pathological evaluation, TB-stained semi-thin specimens were useful for morphological characterization of peripheral neurotoxicity. Semi-thin specimens can evaluate the detail of the changes, including the location, whether axons or myelin sheaths. Even if semi-thin specimens are not available, LFB-Bodian staining can also distinguish axons and myelin sheaths to some extent. The assessment of semi-thin specimens is more sensitive than that of FFPE specimens, because an increase in myelin ovoids could be detected even in the low-dose group on Day 4, when no findings were observed in FFPE specimens. However, the assessment of semi-thin specimens must be combined with FFPE specimens because the evaluation area in semi-thin specimens is very narrow.

In the image analysis, we could show the pathological features objectively as data that are easily understood by non-pathologists by showing the G-ratio as a histogram. Since pathological evaluation is subjective, it is desirable to use an objective index. While the usefulness of image analysis in pathological evaluation has been reported frequently not only in clinical field but also in non-clinical toxicity field in recent years[29-31], this study is one example to demonstrate the

usefulness of image analysis for neurotoxicity. For image analysis, we suggest that data showing the validity of the image recognition used for analysis should be handled as validation data. In drug development, it is particularly important to demonstrate the validity of image analysis when we obtain data to be used for new drug applications, and standardization of how to validate the image analysis will be required in the future[32].

In addition, ChAT immunostaining of FFPE specimens revealed that no nerve fiber degeneration was observed in ChAT-positive motor neurons. The saphenous nerve, contains only somato-sensory fibers in rats[33], was affected similarly to the sciatic nerve. These results suggested that INH-induced peripheral neurotoxicity occurs primarily in sensory nerves, although it had been unclear whether INH-induced peripheral neurotoxicity is primarily located in sensory or motor nerves[16, 21-23]. This is consistent with the clinical signs that begin with sensory abnormalities in feet[24-25]. Differentiation of motor and sensory nerves is important to characterize the pathology and investigate monitoring methods in humans. Although ChAT is used mainly for staining of nerve cell bodies in the CNS, our results showed that ChAT can also objectively distinguish motor and sensory neurons in peripheral nerves on tissue sections.

When combined with pathological results, the usefulness of Nf-L as a peripheral neurotoxic BM mentioned in Chapter 2 is strongly suggested for the detection of nerve fiber injury. Serum Nf-L levels were higher on Day 4 than on Day 9, the time of the most prominent peripheral nerve injury,

suggesting that more Nf-L leaked in the early phase of the injury. On Day 4, the serum Nf-L levels were also high in the low-dose group with minor changes that are difficult to detect by observation of FFPE sections, suggesting that Nf-L is a useful humoral BM that can sensitively detect minor lesions that cannot be detected by observation of FFPE sections. We had assumed that the serum Nf-L levels would increase concurrently with the pathological changes, because Nf-L is a neuronal protein component. In previous studies, serum Nf-L levels were high when peripheral nerve lesions induced by hyperpyridoxine and paclitaxel were prominent[12-13], and gradually increased during vincristine and cisplatin dosing and peaked at the final time point[11-12]. Interestingly, our results showed that the time of the highest peak in Nf-L was earlier than that of the pathological change. Since serum Nf-L measurement could detect changes earlier than pathology, it would be very useful as BMs for peripheral neurotoxicity considering their utilization for toxicity monitoring in humans[34].

Figures and Tables

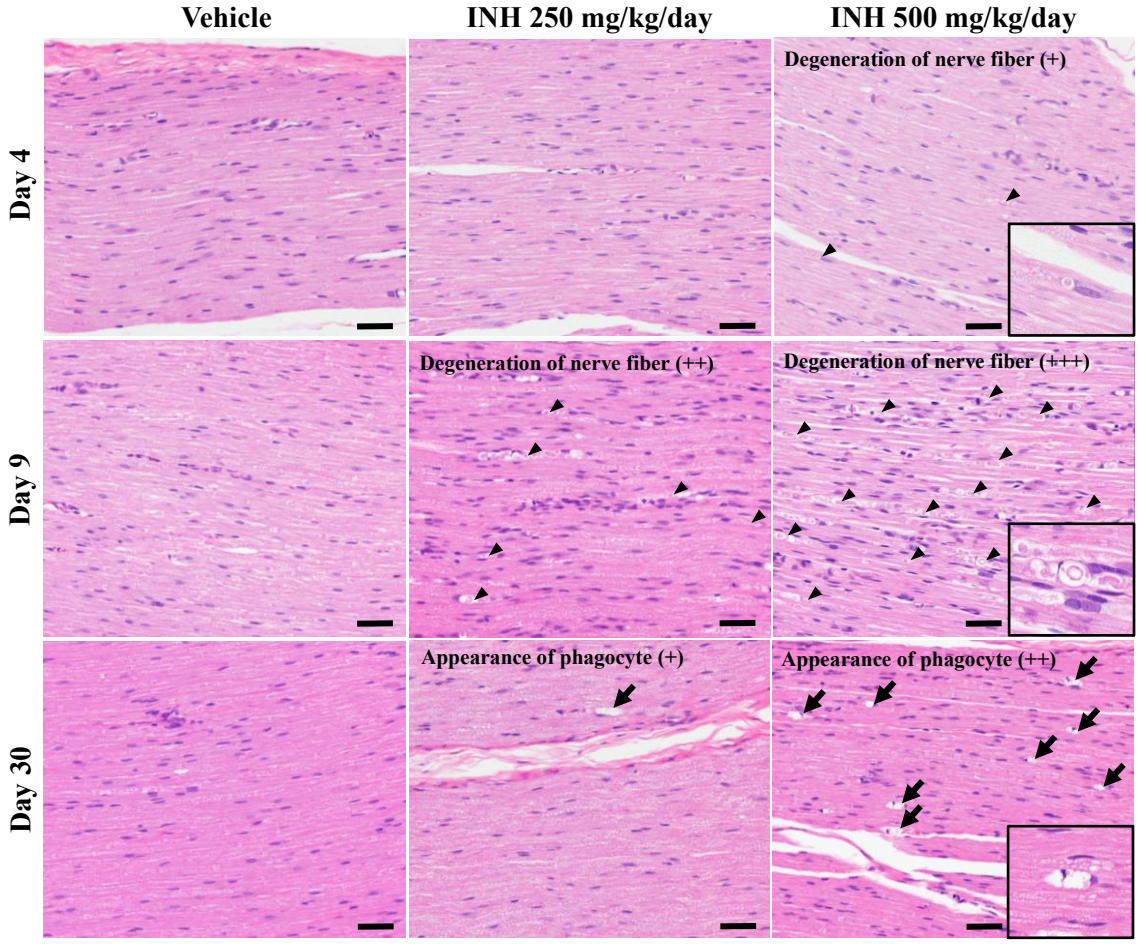

Figure 6. Histopathology of the sciatic nerve in formalin-fixed paraffin-embedded sections. Hematoxylin and eosin staining. In isoniazid (INH) treatment groups, nerve fiber degeneration was observed in some nerve fibers on Day 4, became most significant by Day 9, and recovered by Day 30 (arrowhead). The frequency of the change increased in a dose-dependent manner. On Day 30, foamy cells were observed (arrow). Scale bar = 50 μm.

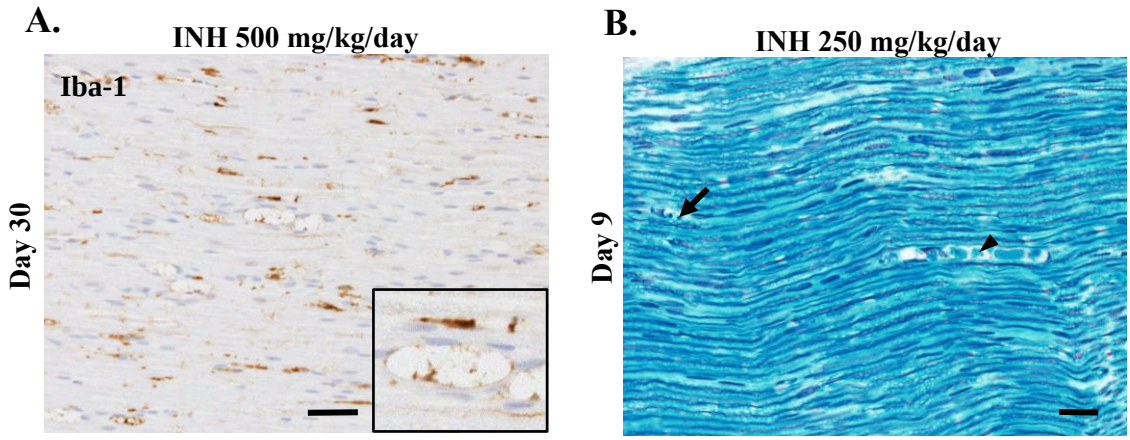

Figure 7. A: Immunohistochemistry for Iba1. The foamy cells were positive for Iba1. Scale bar = 50 µm. B: Luxol Fast Blue-Bodian staining of the sciatic nerve on Day 9 in the low-dose group. Nerve fiber degeneration was observed to be "digestion chambers" with axon fragmentation (arrow) and spherules derived from the myelin sheath (arrowhead). Scale bar = 20 µm.

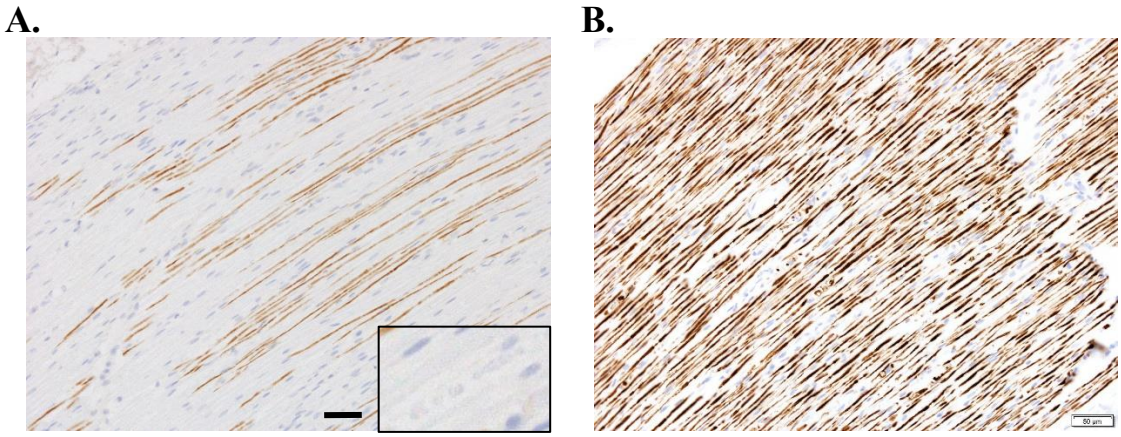

Figure 8. Immunohistochemistry for choline acetyltransferase (ChAT) in formalin-fixed paraffin-embedded longitudinal sections of the sciatic nerve. The images on Day 9 in the high-dose group are shown. ChAT was positive for axons of motor and autonomic neurons (A). Nf-L was positive in all axons, and numerous degenerated nerve fibers are observed (B). No nerve fiber degeneration was observed in the ChAT-positive nerve fibers (A insert). Scale bar = 50 µm..

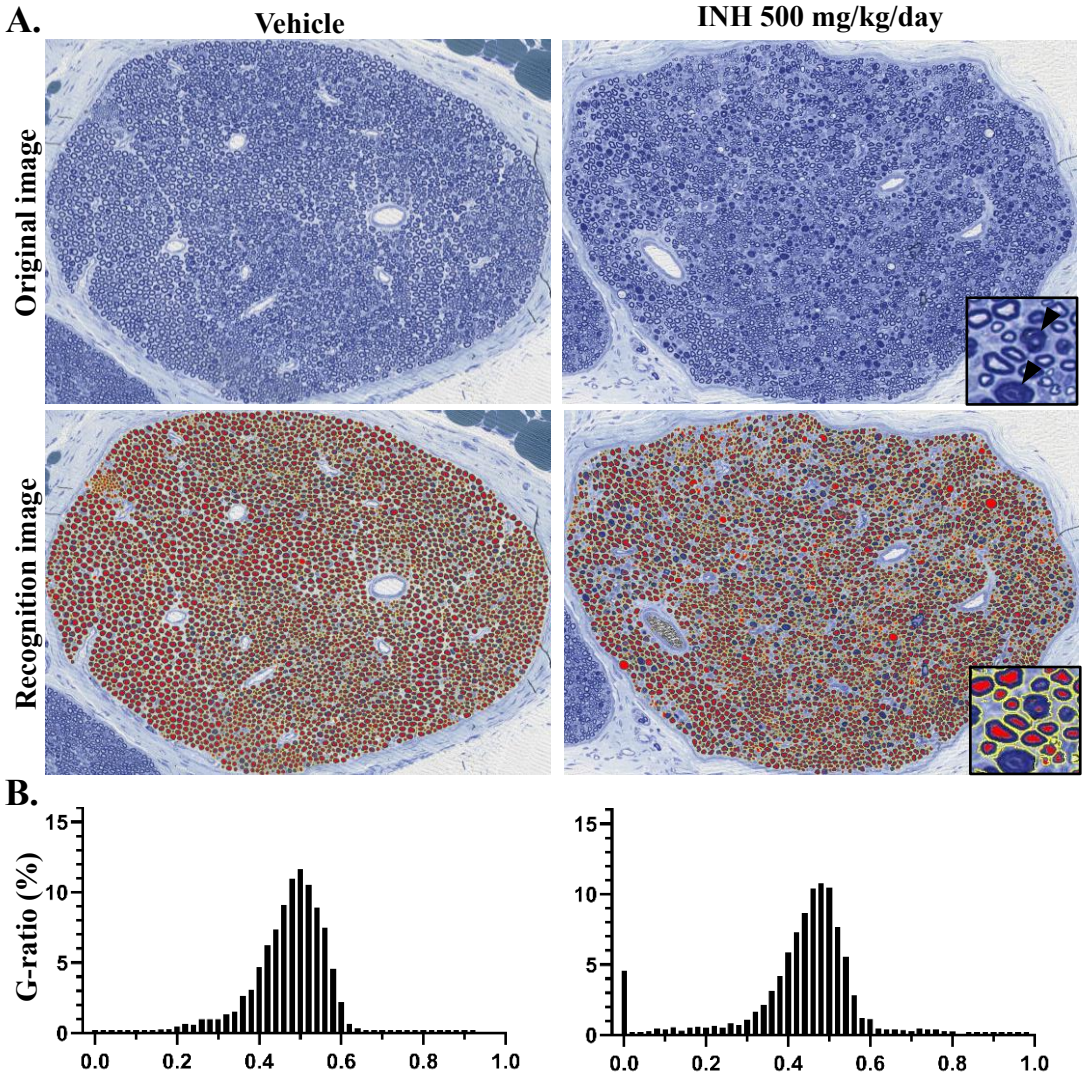

Figure 9. A: Representative toluidine blue-stained semi-thin specimens of the sciatic nerve on Day 9. The sciatic nerve of a rat treated with high-dose isoniazid (INH) showed a marked increase in myelin ovoids (arrowhead), and size differences in nerve fiber diameter. The images after recognition by the axon module of the HALO software were also presented. Nerve fibers are surrounded by yellow lines, and axons are painted red. B: The G-ratio (axon diameter/nerve fiber diameter) was calculated for each nerve fiber, and its distribution was shown as a histogram. In the histogram of a rat treated with high-dose INH compared to that of a vehicle received rat, a marked increase in the G-ratio 0 value was noted. In addition, the variability in nerve fibers was shown as a decrease of the G-ratio distribution and a slight increase in the G-ratio 0.6–0.8 value.

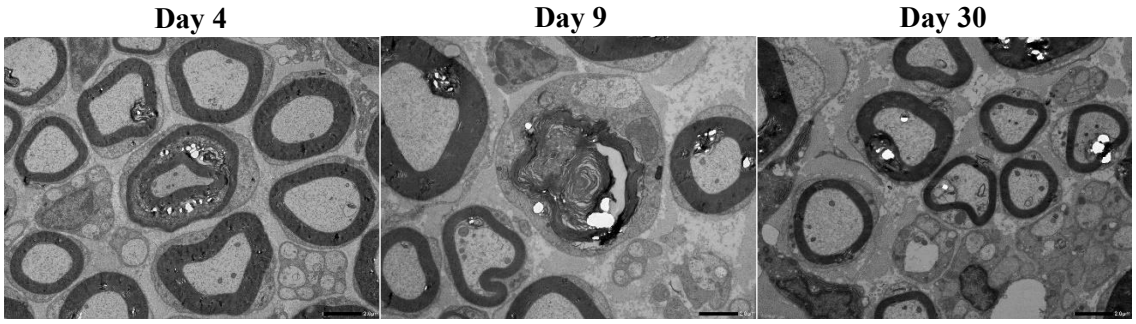

Figure 10. Ultrastructural observation of the sciatic nerve in the high-dose isoniazid group. Representative images are shown. On Day 4, disruption of axon and myelin sheath were observed as early signs of axonal injury. On Day 9, axonal degeneration, disruption of myelin sheath, and myelin ovoid formation were observed in many nerve fibers, accompanied by enlargement of Schwann cells. On Day 30, the frequency of small nerve fibers with thin myelin sheaths was increased. Scale bar = 2 μm.

Table 3. Histopathological findings of FFPE sections for each peripheral nerve.

Findings	Day 4			Day 9			Day 30		
Tissues	Vehicle	INH low	INH high	Vehicle	INH low	INH high	Vehicle	INH low	INH high
Degeneration of nerve fiber									
Sciatic nerve	-	-	+ (3/5)	-	+ (4/5), ++ (1/5)	++ (3/5), +++ (2/5)	-	-	-
Tibial nerve	-	-	+ (2/5)	-	+ (2/5), ++ (3/5)	+++ (5/5)	-	-	+ (1/5)
Saphenous nerve	-	-	+ (2/5)	-	+ (3/5), ++ (2/5)	++ (1/5), +++ (4/5)	-	-	-
Appearance of phagocyte									
Sciatic nerve	-	-	-	-	-	-	-	-	+ (2/5), ++ (3/5)
Tibial nerve	-	-	-	-	-	-	-	-	+ (4/5)
Saphenous nerve	-	-	-	-	-	-	-	-	+ (2/5)

Descriptions in parentheses: number of animals with findings/number of animals examined.
INH low: INH 250 mg/kg/day for 3 days, INH high: INH 500 mg/kg/day for 3 days.
-: no noteworthy findings, +: mild, ++: moderate, +++: severe.

Table 4. Light microscopic findings in the TB-stained semi-thin sections for sciatic nerve.

Findings	Day 4			Day 9			Day 30		
	Vehicle	INH low	INH high	Vehicle	INH low	INH high	Vehicle	INH low	INH high
Myelin ovoid, appearance	-	+ (1/5)	+ (2/5)	-	+ (3/5)	++ (4/5), +++ (1/5)	-	-	-
Shrunken axon	-	-	-	-	-	+ (5/5)	-	-	-
Increase, Schwann cell	-	-	-	-	-	+ (2/5)	-	-	-
Increase, small myelinated fiber	-	-	-	-	-	-	-	-	+ (2/5)

Descriptions in parentheses: number of animals with findings/number of animals examined.
INH low: INH 250 mg/kg/day for 3 days, INH high: INH 500 mg/kg/day for 3 days.
-: no noteworthy findings, +: mild, ++: moderate, +++: severe.

Supplementary Table 2. The validity of image recognition using HALO software

Subject		Number of nerve fibers			Results	
Animal #	Area #	A: Correctly recognized nerve fiber	B: Misrecognition of another tissue as a nerve fiber	C: Failure to recognize nerve fiber	A/(A+B): Positive predictive value	A/(A+C): Sensitivity
10402	1	299	0	11	1	0.9645
	2	320	0	21	1	0.9384
	3	352	0	23	1	0.9387
10602	1	302	7	29	0.9773	0.9124
	2	344	11	32	0.969	0.9149
	3	268	7	15	0.9745	0.947

Validity was confirmed by calculating the positive predictive value and sensitivity. A square of 125 μm^2 was randomly extracted from 3 sites/animal, and nerve fibers were counted visually.

Conclusion

In this study, we assessed peripheral neurotoxicity in INH-treated rats using a combination of evaluations to determine the optimal assessment method for the characterization of peripheral neurotoxicity. There was a discrepancy between the time points of marked pathological changes and the changes in biochemical and behavioral assessments, suggesting the importance of setting multiple necropsy time points and combining each evaluation. Although pathological evaluation is essential for pathological characterization, the results of biochemical and behavioral assessments at the same time points as the pathological evaluation are valuable. In this study, using an INH-induced peripheral neuropathy rat model, we found that serum Nf-L measurement could detect changes earlier than pathology, indicating it would be very useful as a BM for peripheral neurotoxicity. Moreover, the observation of semi-thin specimens and ChAT immunostaining were useful for characterizing morphological neurotoxicity, and image analysis of semi-thin specimens enabled us to objectively show pathological features. In order to generalize our approach, further evaluation in any peripheral neurotoxic model will be required.

Table 5. Summary of the results of each evaluation. Advantages and disadvantages identified from the results are noted. Toxicologically significant changes are highlighted in gray.

			Results									Discussion	
			Vehicle	INH low	INH high	Vehicle	INH low	INH high	Vehicle	INH low	INH high	Usefulness of the endpoints	
Assessment		Findings	Days 3–5			Days 8–9			Day 30			Advantages	Disadvantages
Behavioral assessment	Ipsilateral flexor reflex (one of the Irwin's test) [a]	Mild hyporeflexia of the hindlimb	-	-	P (3/15) [b]	-	-	-	-	-	-	- High sensitivity: Behavioral abnormalities not detected in general clinical signes were detected - Easy to include in toxicity studies: Easy to assess and low stress on animals	- Causes of abnormal movements cannot be identified
	Thermal sensitivity test (hotplate method) [c]	Delayed time from placement on a hot plate to evading behavior	-	-	P (2/15)	-	-	-	NA	NA	NA	- High sensitivity: Behavioral abnormalities not detected in general clinical signes were detected	- Difficult to judge by subjective observation - Too much time for acclimatization and evaluation - Unable to detect sensory abnormalities other than thermal stimuli
Assessment			Day 4			Day 9			Day 30			Advantages	Disadvantages
Bioanalysis	Serum Nf-L (pg/mL)		17.6±6.30 (n=4)	143±180 (n=5) [d]	813±909 (n=4) [d]	7.79±0.88 (n=3)	23.1±21.2 (n=5)	128±69.6 (n=5)**	5.99±1.21 (n=3)	NA	10.1±4.05 (n=5)	- High sensitivity and early detectivity: Even minor changes difficult to note by pathology became high value - Less invasivity	- High inter-individual variability - Less specificity: Nf-L is a constituent protein in nerve tissue and cannnot specify which nerve tissue is damaged
	Plasma PL (nM)		611±183 (n=5)	106±48.2 (n=5)***	60.1±23.7 (n=5)***	583±59.8 (n=5)	624±219 (n=5)	563±195 (n=5)	415±92.3 (n=5)	481±125 (n=5)	395±55.0 (n=5)	- Useful for mechanistic discussion	- Difficult to measure: Some endogenous molecules - Unable to determine what to measure if a mechanistic hypothesis cannot be developed
	Plasma PLP (nM)		803±131 (n=5)	137±44.9 (n=5)***	35.8±8.41 (n=5)***	759±37.8 (n=5)	637±75.4 (n=5)* [e]	727±92.2 (n=5)	796±121 (n=5)	822±116 (n=5)	734±118 (n=5)		
Assessment		Findings	Day 4			Day 9			Day 30			Advantages	Disadvantages
Pathology	FFPE specimens, HE stain (sciatic nerve)	Degeneration of nerve fiber	-	-	+ (3/5)	-	+ (4/5), ++ (1/5)	++ (3/5), +++ (2/5)	-	-	-	- Wide evaluation area: especially longitudinal - Able to compare changes in multiple nerves	- Inability to distinguish detailed features
		Appearance of phagocyte	-	-	-	-	-	-	-	-	+ (2/5), ++ (3/5)		
	Semi-thin specimens, TB stain (sciatic nerve)	Myelin ovoid, appearance	-	+ (1/5)	+ (2/5)	-	+ (3/5)	++ (4/5), +++ (1/5)	-	-	-	- Pathologic characterization: Axons or myelin sheaths - High sensitivity: Findings detected at low dose on Day 4	- Small evaluation area
		Shrunken axon	-	-	-	-	-	+ (5/5)	-	-	-		
		Increase, Schwann cell	-	-	-	-	-	+ (2/5)	-	-	-		
		Increase, small myelinated fiber	-	-	-	-	-	-	-	-	+ (2/5)		

Descriptions in parentheses: number of animals with findings/number of animals examined.
INH low, isoniazid 250 mg/kg/day for 3 days; INH high, isoniazid 500 mg/kg/day for 3 days; Nf-L, neurofilament light chain; PL, pyridoxal, PLP, pyridoxal phosphate; FFPE, formalin-fixed paraffin-embedded; HE, hematoxylin and eosin; TB, toluidine blue;
-, no noteworthy findings; P, present; +, mild; ++, moderate; +++, severe; NA, not appreciable.
Dunnett's multiple comparison test: *$P < 0.05$ versus control, **$P < 0.01$ versus control, ***$P < 0.001$ versus control.
a: Ipsilateral flexor reflex was examined on Days 3–6, 8–9, and 30.
b: Mild hyporeflexia of the hind limb was noted in 3 of 15 animals on Day 4, and in 1 of 10 animals on day 5. It was not noted on Day 3 and after Day 6.
c: Thermal sensitivity test was performed on Days 3 and 8.
d: The increases were considered toxicologically significant treatment-related changes, because multiple animals were noted at a clearly high level that does not occur normally, regardless of no statistical significance.
e: The decrease was not considered a treatment-related change, because it was a mild decrease and not noted in the high-dose group, regardless of statistical significance.

Reference

1. OECD. Guidance document for neurotoxicity testing. OECD Environment, Health and Safety Publications Series on Testing and Assessment, No. 20. Paris. 2004.

2. OECD. Neurotoxicity study in rodents. OECD Guideline for the Testing of Chemicals, No. 424. Paris. 1997.

3. EPA. Neurotoxicity screening battery. Health Effects Test Guidelines, OPPTS 870.6200. Washington DC. 1998.

4. Bolon B, Krinke G, Butt MT, Rao DB, Pardo ID, Jortner BS, Garman RH, Jensen K, Andrews-Jones L, Morrison JP, Sharma AK, and Thibodeau MS. STP position paper: Recommended best practices for sampling, processing, and analysis of the peripheral nervous system (nerves and somatic and autonomic ganglia) during nonclinical toxicity studies. Toxicol Pathol. 46: 372–402. 2018.

5. Buruna J, Alberti P, Calls-Cobos A, Caillaud M, Damaj MI, and Navarro X. Methods for in vivo studies in rodents of chemotherapy induced peripheral neuropathy. Exp Neurol. 325: 113154. 2020.

6. Bonomo R and Cavaletti G. Clinical and biochemical markers in CIPN: A reappraisal. Rev Neurol (Paris). 177: 890–907. 2021.

7. Coppens S, Lehmann S, Hopley C, and Hirtz C. Neurofilament-light, a promising biomarker: analytical, metrological and clinical challenges. 24: 11624. 2023.

8. Alcolea D, Beeri MS, Rojas JC, Gardner RC, and Lleó A. Blood biomarkers in neurodegenerative diseases: implications for the clinical neurologist. Neurology. 101: 172–180. 2023.

9. Arslan B and Zetterberg H. Neurofilament light chain as neuronal injury marker - what is needed to facilitate implementation in clinical laboratory practice? Clin Chem Lab Med. 61: 1140–1149. 2023.

10. Rossor AM and Reilly MM. Blood biomarkers of peripheral neuropathy. Acta Neurol Scand. 146: 325–331. 2022.

11. Meregalli C, Fumagalli G, Alberti P, Canta A, Carozzi VA, Chiorazzi A, Monza L, Pozzi E, Sandelius Å, Blennow K, Zetterberg H, Marmiroli P, and Cavaletti G. Neurofilament light chain as disease biomarker in a rodent model of chemotherapy induced peripheral neuropathy. Exp Neurol. 307: 129–132. 2018.

12. Meregalli C, Fumagalli G, Alberti P, Canta A, Chiorazzi A, Monza L, Pozzi E, Carozzi VA, Blennow K, Zetterberg H, Cavaletti G, and Marmiroli P. Neurofilament light chain: a specific serum biomarker of axonal damage severity in rat models of Chemotherapy-Induced Peripheral Neurotoxicity. Arch Toxicol. 94: 2517–2522. 2020.

13. Sano T, Masuda Y, Yasuno H, Shinozawa T, Watanabe T, and Kakehi M. Blood neurofilament light chain as a potential biomarker for central and peripheral nervous toxicity in rats. Toxicol Sci. 185: 10–18. 2021.

14. Badrinath M and John S. Isoniazid toxicity. 2022, from StatPearls Publishing website: https://www.ncbi.nlm.nih.gov/books/NBK531488

15. Hadtstein F and Vrolijk M. Vitamin B-6-induced neuropathy: exploring the mechanisms of pyridoxine toxicity. Adv Nutr. 12: 1911–1929. 2021.

16. Reddy P. Preventing vitamin B6-related neurotoxicity. Am J Ther. 29: e637–e643. 2022.

17. Chua CL, Ohnishi A, Tateishi J, and Kuroiwa Y. Morphometric evaluation of degenerative and regenerative changes in isoniazid-induced neuropathy. Acta Neuropathol. 60: 183–193. 1983.

18. Ohnishi A, Chua CL, and Kuroiwa Y. Axonal degeneration distal to the site of accumulation of vesicular profiles in the myelinated fiber axon in experimental isoniazid neuropathy. Acta Neuropathol. 67: 195–200. 1985.

19. Schalaepfer WW and Hager H. Ultrastructural Studies of INH-induced neuropathy in rats. 1. Early axonal changes. Am J Pathol. 45: 209–219. 1964.

20. Schalaepfer WW and Hager H. Ultrastructural Studies of INH-induced neuropathy in rats. 3. Repair and regeneration. Am J Pathol. 45: 679–689.1964.

21. Jacobs JM, Miller RH, and Cavanagh JB. The distribution of degenerative changes in INH neuropathy. Further evidence for focal axonal lesions. Acta Neuropathol. 48: 1–9. 1979.

22. Arsalan R and Sabzwari S. Isoniazid induced motor-dominant neuropathy. J Pak Med Assoc. 65: 1131–1133. 2015.

23. Argov Z and Mastaglia FL. Drug-induced peripheral neuropathies. Br Med J. 1: 663–666. 1979.

24. Aita JF and Calame TR. Peripheral neuropathy secondary to isoniazid-induced pyridoxine deficiency. Md State Med J. 21: 68–70. 1972.

25. Steichen O, Martinez-Almoyna L, and Broucker TD. Isoniazid induced neuropathy: consider prevention. Rev Mal Respir. 23: 157–160. 2006.

26. Deus JR, Dvorakova LS, and Vetter I. Methods Used to Evaluate Pain Behaviors in Rodents. Front Mol Neurosci. 10: 284. 2017.

27. Mathiasen JR and Moser VC. The Irwin Test and Functional Observational Battery (FOB) for Assessing the Effects of Compounds on Behavior, Physiology, and Safety Pharmacology in Rodents. Curr Protoc. 3: e780. 2023.

28. Ugrenović S, Jovanović I, Vasović L, Kundalić B, Čukuranović R, and Stefanović V. Morphometric analysis of the diameter and g-ratio of the myelinated nerve fibers of the human sciatic nerve during the aging process. Anat Sci Int. 91: 238–245. 2016.

29. Horai Y, Kakimoto T, Takemoto K, and Tanaka M. Quantitative analysis of histopathological findings using image processing software. J Toxicol Pathol. 30: 351–358. 2017.

30. Horai Y, Mizukawa M, Nishina H, Nishikawa S, Ono Y, Takemoto K, and Baba N. Quantification of histopathological findings using a novel image analysis platform. J Toxicol Pathol. 32: 319–327. 2019.

31. Hwang J, Lim M, Han G, Park H, Kim Y, Park J, Jun S, Lee J, and Cho J. A comparative study on the implementation of deep learning algorithms for detection of hepatic necrosis in toxicity studies. Toxicol Res. 39: 399–408. 2023.

32. Bankhead P. Developing image analysis methods for digital pathology. J Pathol. 257: 391–402. 2022.

33. Campos SAR, Sanada LS, Sato KL and Fazan VPS. Morphometry of saphenous nerve in young rats. J Neurosci Methods. 168: 8–14. 2008.

34. Fundaun J, Kolski M, Molina-Álvarez M, Baskozos G, and Schmid AB. Types and concentrations of blood-based biomarkers in adults with peripheral neuropathies: a systematic review and meta-analysis. JAMA Network Open. 5: 32248593. 2022.

Acknowledgement

The author wishes to his sincere appreciation and gratitude to Prof. Junichi Kamiie, Professor of Veterinary Pathology, Azabu University, for his valuable guidance and encouragement for 4 years, as well as critical review of this thesis, as a supervisor. The author sincerely thanks Dr. Naoyuki Aihara and Dr. Takanori Shiga, Veterinary Pathology, Azabu University, for their valuable advice and encouragement for 4 years.

The author also thanks to Prof. Motoharu Sakaue, Laboratory of Anatomy II, Azabu University, and Prof. Kensuke Orito, Laboratory of Phisiology II, Azabu University, for their kind advice. I would also like to thank Prof. Emer. Kinji Shirota, Veterinary Pathology, Azabu University, and Prof. Emer. Yumi Une, Veterinary Pathology, Okayama University of Science, for their pathological education.

This study was supported by many colleagues, Safety Research Laboratory, Mitsubishi Tanabe Pharma Corporation. The author especially thankful to Dr. Satomi Nishikawa, Dr. Tetsuya Sakairi, Ms. Mao Mizukawa, Dr. Hironobu Nishina, and Mr. Katsuya Fujiki for their pathological support. The author also especially thankful to Mr. Yuhei Ozawa, Dr. Yui Hibino, and Mr. Takashi Tateoka for the technical support with their specialty.

Thanks are also due to all graduate and undergraduate students of the author's laboratory, especially Ms. Mao Mizukawa, Ms. Yumiko Kamiya, and Mr. Yu Uchida for their kind advice

and friendly support.

A part of this thesis was published as a following article.

1. Kashimura, A., Nishikawa, S., Ozawa, Y., Hibino, Y., Tateoka, T., Mizukawa, M., Nishina, H., Sakairi, T., Shiga, T., Aihara, N., and Kamiie, J.: Combination of pathological, biochemical and behavioral evaluations for peripheral neurotoxicity assessment in isoniazid-treated rats. *Journal of Toxicologic Pathology*, Apr;37(2):69-82, 2024.